Available online at www.sciencedirect.com
SCIENCE DIRECT®
International Journal of Mass Spectrometry 228 (2003) 797–805
International Journal of Mass Spectrometry
www.elsevier.com/locate/ijms

Collision-induced symmetric fission of doubly-charged cubelike $[Fe_4S_4X_4]^{2-}$ clusters

Xin Yang [a,b], Xue-Bin Wang [a,b], Lai-Sheng Wang [a,b,*]

[a] *Department of Physics, Washington State University, 2710 University Drive, Richland, WA 99352, USA*
[b] *W.R. Wiley Environmental Molecular Sciences Laboratory, Pacific Northwest National Laboratory, MS K8-88, P.O. Box 999, Richland, WA 99352, USA*

Received 24 November 2002; accepted 2 April 2003

Dedicated to Prof. Helmut Schwarz.

Abstract

A series of doubly-charged [4Fe4S] cluster ions, $[Fe_4S_4X_4]^{2-}$ (X = Cl, Br, I, and SC_2H_5), were produced in the gas phase by electrospray ionization and examined using collision-induced dissociation (CID) in a quadrupole ion trap. CID channels of each dianion were analyzed by MS/MS experiments at different collision energies. Two CID channels were observed for these dianions: symmetric fission and electron detachment. The most interesting observation is the symmetric fission of $[Fe_4S_4X_4]^{2-}$ into two identical daughter ions, $[Fe_2S_2X_2]^{-}$. The important role of the intramolecular coulomb repulsion in the symmetric fission was shown by comparing with CID of the singly-charged anions, $[Fe_4S_4X_4]^{-}$. Our gas-phase experiments suggest that solution phase conversions between $[Fe_4S_4]$ and $[Fe_2S_2]$ assemblies in proteins may also involve related fission chemistry with reactive $[Fe_2S_2X_2]^{-}$ intermediates.

Keywords: Ion fission; Iron–sulfur clusters; Collision-induced dissociations; Multiply-charged anions; Electrospray

1. Introduction

Iron–sulfur proteins are ubiquitous in living matters and usually contain iron–sulfur clusters with one, two, or four iron atoms. The most common and representative active site of these proteins is composed of the [4Fe4S] cluster, such as those in the bacterial ferredoxins (Fds) and the high potential iron sulfur proteins (HiPIP) [1–7]. In this cubelike cluster, each iron atom is approximately tetrahedrally coordinated to three inorganic μ_3-sulfur ions and to one external sulfur from a cysteine amino acid, as schematically shown in Fig. 1. Many model systems of the $[Fe_4S_4]$ active site have been developed since the early 1970s by replacing the cysteine ligation with simple thiolate ligands [8–10]. Geometric and electronic structural data confirmed that the synthetic complexes are accurate analogs of the protein-bound sites. Compared with the native Fe–S clusters in proteins, the synthetic analogs can be studied more straightforwardly and can provide more detailed insight into the intrinsic properties of the active sites.

* Corresponding author. Tel.: +1-509-376-8709; fax: +1-509-376-6066.
E-mail address: ls.wang@pnl.gov (L.-S. Wang).

1387-3806/$ – see front matter © 2003 Elsevier Science B.V. All rights reserved.
doi:10.1016/S1387-3806(03)00189-1

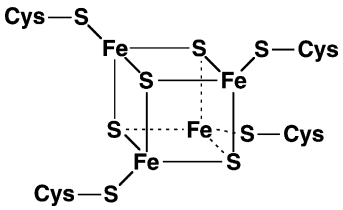

Fig. 1. A schematic structural model of the [4Fe4S] cluster in proteins.

The [4Fe4S] clusters occur naturally in three different oxidation states, $[Fe_4S_4]^{1+}$, $[Fe_4S_4]^{2+}$, and $[Fe_4S_4]^{3+}$. The [4Fe] ferrodoxins operate between the first two redox states, whereas the HiPIPs utilize the 2+/3+ redox couple [11,12]. The $[Fe_4S_4]^{2+}$ center formally consists of 2Fe(III) and 2Fe(II) ions. However, it was found experimentally that all the four iron sites are in the same formal oxidation state, which is generally considered to be $Fe^{2.5+}$ [1]. Broken-symmetry density functional theory (DFT) calculations confirmed this experimental observation by suggesting that the $[Fe_4S_4]^{2+}$ core basically contains two valent-delocalized sub-layers [13–15]. In each sub-layer, the excess electron in the putative Fe(II) site is in fact delocalized over two Fe(III) atoms. The two high spin iron centers are coupled ferromagnetically in each layer while the two layers are coupled antiferromagnetically to give a low spin state ($s = 0$) for the entire $[Fe_4S_4]^{2+}$ cluster.

Iron–sulfur clusters have a remarkable ability for conversion and interconversion in both free and protein-bound conditions. The most common transformation is the interconversion between the cubane $[Fe_4S_4]^{2+}$ and the cuboidal $[Fe_3S_4]^{+}$ observed in the *Desulfovibrio gigas ferredoxin* II and the enzyme aconitase [16,17]. Synthetically, $[Fe_4S_4]^{2+}$ can be obtained through reactions: $2[Fe_2S_2(SR)_4]^{2-} \leftrightarrow 2[Fe_2S_2(SR)_4]^{3-} \rightarrow [Fe_4S_4(SR)_4]^{2-}$ [1]. The first example of a direct $[Fe_4S_4]^{2+} \rightarrow [Fe_2S_2]^{2+}$ conversion in protein was reported in 1984 when the oxidized Fe protein from *Azotobacter vinelandii* nitrogenase was exposed to a chelator (α,α'-dipyridyl) in the presence of MgATP [18]. In 1997, an almost quantitative conversion of $[Fe_4S_4]^{2+}$ to $[Fe_2S_2]^{2+}$ was observed on exposure of the FNR (fumarate nitrate reduction) protein of *Escherichia coli* to dioxygen [19]. This protein is an transcriptional activator that controls numerous genes required for the synthesis of components of the anaerobic respiratory pathways of *E. coli*. When isolated aerobically, FNR is inactive and exists as a 30-kDa monomer. The active protein is dimeric and contains one $[Fe_4S_4]^{2+}$ cluster per subunit [20]. On exposure to dioxygen, these $[Fe_4S_4]^{2+}$ clusters are readily converted to $[Fe_2S_2]^{2+}$ in high yield. The $[Fe_2S_2]^{2+}$ cluster form of FNR is much more stable to oxygen, but was unable to sustain biological activity. The $[Fe_2S_2]^{2+}$ cluster can be largely reconverted to the $[Fe_4S_4]^{2+}$ form on reduction with dithionite in vitro [19]. The same cluster conversion also occurs in vivo on exposure to O_2 [21]. These investigations demonstrate that the $[Fe_4S_4]^{2+} \leftrightarrow [Fe_2S_2]^{2+}$ conversion has important biological implications, but the reaction mechanisms remain unknown.

Electrospray ionization (ESI) is a versatile technique, allowing ionic species, especially multiply-charged anions, in solution samples to be transported into the gas phase. Tandem mass spectrometry techniques (MS/MS or MS^n) can provide detailed structural information about many different types of ions, including those generated from peptides [22–24], proteins [25–30], carbohydrates [31–33], and inorganic clusters [34,35]. Quadrupole ion traps have been used extensively in MS/MS experiments because of their abilities for ion storage and collision-induced dissociation (CID) [36,37]. We are interested in probing the electronic structures of the Fe–S cluster analogs in the gas phase using ESI and photoelectron spectroscopy (PES) [38,39]. Recently, we observed surprisingly symmetric fissions in two [4Fe4S] complexes, $[Fe_4S_4Cl_4]^{2-}$ and $[Fe_4S_4Br_4]^{2-}$ and probed the fission mechanisms using a combination of techniques including CID, PES, and DFT calculations [40]. In the current paper, we report the details of the CID experiments. More importantly, we include the more biologically relevant analog, $[Fe_4S_4(SC_2H_5)_4]^{2-}$, as well as observations on $[Fe_4S_4I_4]^{2-}$. CID channels were analyzed by MS/MS experiments at different collision energies. For the clusters with X = Cl, Br, and SC_2H_5, the dominant CID fragments are the

fission product $[Fe_2S_2X_2]^-$. For $[Fe_4S_4I_4]^{2-}$, the dominant CID channel is electron detachment producing the singly-charged cluster $[Fe_4S_4I_4]^-$. We also speculate on the implications of the gas-phase fission processes for the conversion between $[Fe_4S_4]$ and $[Fe_2S_2]$ assemblies in biological systems.

2. Experimental

A commercial LCQ (Finnigan, San Jose, CA) electrospray/quadrupole ion trap mass spectrometer was employed in the negative spray mode for all the experiments. To produce the anions of interest, $[Fe_4S_4X_4]^{2-}$ (X = Cl, Br, I, and SC_2H_5), we used 10^{-3} M solutions of their corresponding tetrabutylammonium salts in O_2-free acetonitrile. Sample solutions were introduced by a syringe pump at a bias voltage of −4.0 kV. Nitrogen gas was used both as the sheath and auxiliary gas in the electrospray source. The dianions of interest, $[Fe_4S_4X_4]^{2-}$ (X = Cl, Br, I, and SC_2H_5), were first isolated in the trap by ejecting all other anions. After isolation, an excitation AC voltage was applied to the end caps to induce collisions of the isolated anions with the background gas (10^{-4} Torr N_2). The Mathieu parameter q_z value for resonance excitation was 0.25. The ion excitation time for CID was 30 ms. The amplitude of the excitation AC voltage used for CID was optimized in each experiment. It was ramped up as relative collision energy (CE) from 0 to 100%, which corresponded to 0–2.5 V zero-to-peak resonant excitation potential as calibrated by the manufacturer (Finnigan LCQ) The contents of the ion trap were then analyzed to detect the CID products.

3. Results

3.1. CID of $[Fe_4S_4Cl_4]^{2-}$ and $[Fe_4S_4Br_4]^{2-}$: symmetric fission

Mass spectra of isolated $[Fe_4S_4Cl_4]^{2-}$ and $[Fe_4S_4Br_4]^{2-}$ and their CID products are presented in Fig. 2. The symmetric fission was the only CID channel for both dianions at different collision energies, forming two $[Fe_2S_2X_2]^-$ (X = Cl, Br) daughter anions. Surprisingly, no electron detachment or simple ligand loss channels were observed. The fission products $[Fe_2S_2X_2]^-$, which have the same mass-to-charge (m/z) ratios as the parent dianions, can be identified easily by the isotope patterns. The single mass peak isolated for $[Fe_4S_4Cl_4]^{2-}$ (Fig. 2a) was mainly due to the isotopmer $[Fe_4S_4{}^{35}Cl_3{}^{37}Cl]^{2-}$ (m/z = 247). It split into two dominating isotopic combinations, $[Fe_2S_2{}^{35}Cl_2]^-$ (m/z = 246) and $[Fe_2S_2{}^{35}Cl{}^{37}Cl]^-$ (m/z = 248) in the CID products (Fig. 2b). The parent dianion peak (m/z = 247) was almost invisible in the CID mass spectrum even at the threshold CE of 20 (Fig. 2b), suggesting that the fission channel is very efficient. At a higher collision energy (Fig. 2c), the CID spectrum did not change much, implying that the fission product, $[Fe_2S_2Cl_2]^-$, was relatively stable. The CID behavior of $[Fe_4S_4Br_4]^{2-}$ (Fig. 2d–f) was identical to that of $[Fe_4S_4Cl_4]^{2-}$. The isolated isotopic peak was $[Fe_4S_4{}^{79}Br_2{}^{81}Br_2]^{2-}$ (m/z = 336), from which three fission isotopmers were observed: $[Fe_2S_2{}^{79}Br_2]^-$ (m/z = 334), $[Fe_2S_2{}^{79}Br{}^{81}Br]^-$ (m/z = 336), and $[Fe_2S_2{}^{81}Br_2]^-$ (m/z = 338) (Fig. 2e). The observed $[Fe_4S_4Cl_3O_2]^-$ and $[Fe_4S_4Br_3O_2]^-$ mass signals were due to ligand exchange reactions with residual background O_2 during the CID processes. It appeared that this reactive channel was very efficient for $[Fe_4S_4Br_4]^{2-}$, because the product, $[Fe_4S_4Br_3O_2]^-$, dominated the CID spectra (Fig. 2e and f).

3.2. CID of $[Fe_4S_4(SEt)_4]^{2-}$

The CID spectra of $[Fe_4S_4(SEt)_4]^{2-}$ were much more complicated and strongly CE dependent, as shown in Fig. 3. We isolated the major isotopmer of $[Fe_4S_4(SEt)_4]^{2-}$ at m/z = 298, and began to observe CID products at a threshold of CE = 20. The CID product at m/z = 596 was from a new channel, i.e., the collision-induced electron detachment of $[Fe_4S_4(SEt)_4]^{2-}$. The two weak peaks emerging from the sides of the parent dianions at m/z = 296 and 299 were due to isotopmers of the symmetric fission

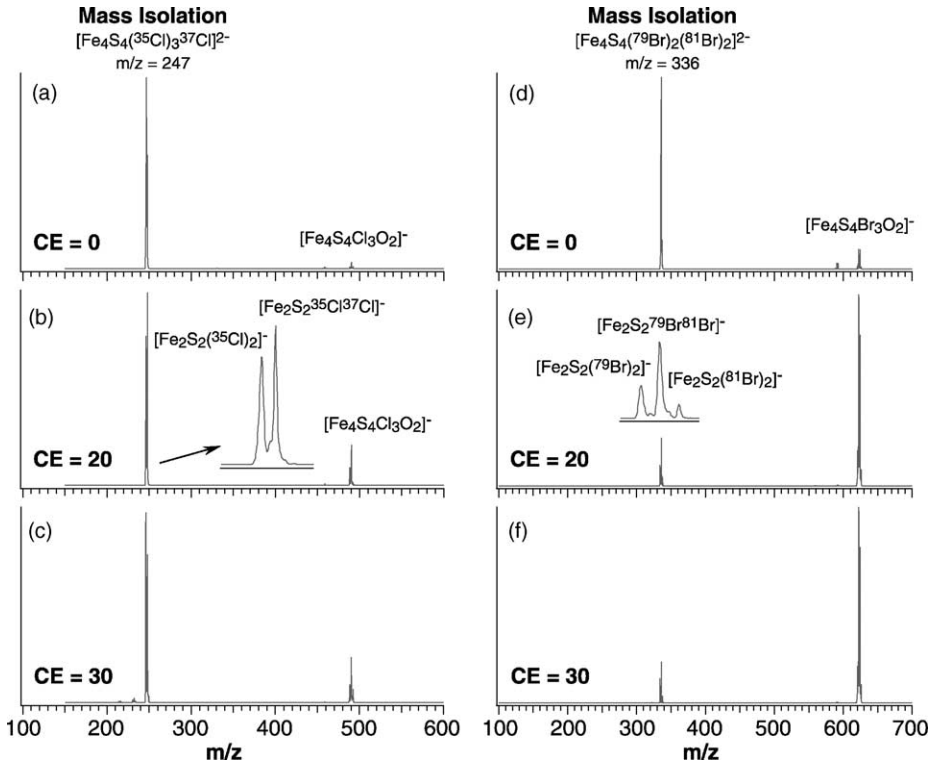

Fig. 2. Collision-induced dissociation (CID) of mass-selected anions of $[Fe_4S_4Cl_4]^{2-}$ and $[Fe_4S_4Br_4]^{2-}$ each at two different collision energies. Ligand exchange reaction with residual background O_2 was observed during the CID experiments. All CID fragments were confirmed by their appropriate isotope patterns as shown.

product $[Fe_2S_2(SEt)_2]^-$. Their small relative intensities indicate that most of the parent dianions remained undissociated at this collision energy. At CE = 25, the relative intensities of these two isotopic peaks increased considerably, suggesting a complete dissociation of the parent dianions. Three small fragments were observed and identified as $[Fe_2S_2(SEt)S]^-$, $[Fe_2S_2(SEt)]^-$, and $[FeS(SEt)_2]^-$ even at the threshold collision energy of CE = 20. Their relative intensities exhibited strong CE dependence and became the dominant CID products at high CE (Fig. 3d). We should point out that, unlike $[Fe_4S_4Cl_4]^{2-}$ and $[Fe_4S_4Br_4]^{2-}$, for which a single isotopmer of the doubly-charged anion could be isolated, the $m/z = 298$ mass peak isolated for $[Fe_4S_4(SEt)_4]^{2-}$ has identical m/z as the fission product, $[Fe_2S_2(SEt)_2]^-$. However, the isotope pattern in the CID spectra and the observation of the electron loss channel in the CID, as well as our PES data, showed that the $[Fe_2S_2(SEt)_2]^-$ ion was less than 10% in the initially isolated $m/z = 298$ peak (Fig. 3a) in the CID experiment of $[Fe_4S_4(SEt)_4]^{2-}$.

3.3. CID of singly-charged [4Fe4S] complexes

Fig. 4 shows the full mass spectrum from the LCQ mass spectrometer by spraying a CH_3CN solution of $(BTBA)_2[Fe_4S_4I_4]$ (BTBA: benzyl-tri-*n*-butylammonium). Only the singly-charged parent anion $[Fe_4S_4I_4]^-$ and the ligand exchange product $[Fe_4S_4I_3O_2]^-$ were observed. The parent dianion $[Fe_4S_4I_4]^{2-}$ was absent in this mass spectrum, but it was observed in our home-built ESI-TOF-PES apparatus [41]. This was due to the fact that in the LCQ apparatus there were more molecular collisions during the ion transport and storage even at CE = 0 in the trap. Collision-induced dissociation or electron

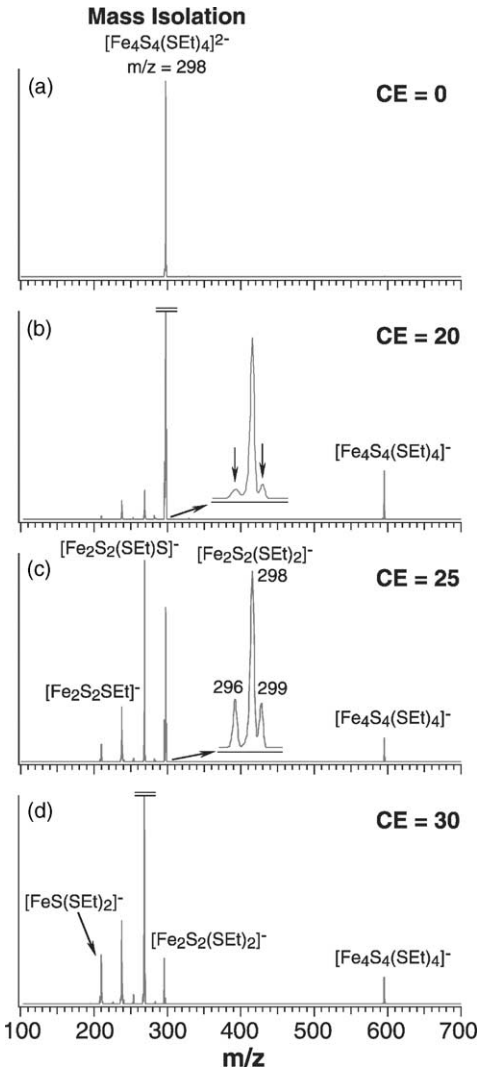

Fig. 3. CID of mass-selected $[Fe_4S_4(SEt)_4]^{2-}$ at three different collision energies. The opening of the symmetric fission channel can be recognized easily by the isotopic peaks of the fission product as shown in (b) and (c).

detachment could occur if the activation barrier is low enough to be overcome by collisions with the background gas during ion transport and storage.

Besides $[Fe_4S_4I_4]^-$, singly-charged $[Fe_4S_4X_4]^-$ anions were present in the mass spectra of all the [4Fe4S] samples. Analogous to $[Fe_4S_4I_4]^-$, these singly-charged species could be due to collision-induced electron detachment of the parent dianions

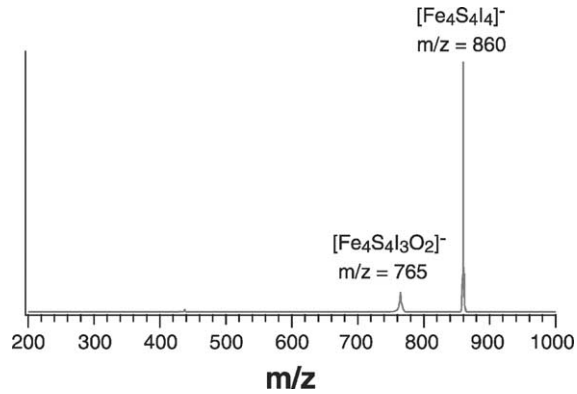

Fig. 4. Mass spectrum from the LCQ mass spectrometer by spraying a $(BTBA)_2[Fe_4S_4I_4]^{2-}$ sample solution. Note the absence of the $[Fe_4S_4I_4]^{2-}$ doubly-charged anion due to collision-induced electron detachment during ions transport and storage.

during ion transport and storage. However, we did not observe any electron loss channel in the CID experiments for $[Fe_4S_4Cl_4]^{2-}$ and $[Fe_4S_4Br_4]^{2-}$, indicating that the singly-charged anions might be also present in the solution samples due to oxidation by O_2. We performed CID experiments for some of these singly-charged anions, as shown in Fig. 5. For $[Fe_4S_4Cl_4]^-$, the only CID fragment, $[Fe_3S_4Cl_2]^-$, was due to the loss of one Fe^{2+} and two Cl^- at a very high collision energy of CE = 35 (Fig. 5a). Much more CID channels were opened for $[Fe_4S_4(SEt)_4]^-$ and most of the CID products were due to ligand (–SEt or –Et) loss or loss of a μ_3-S. The only CID product for $[Fe_4S_4I_4]^-$ was the ligand loss product $[Fe_4S_4I_3]^-$, which appeared to have reacted overwhelmingly with the residual background O_2 forming the strong mass signal of $[Fe_4S_4I_3O_2]^-$. Interestingly, we observed no symmetric fission to give the [2Fe2S] products in the CID of all the singly-charged anions.

4. Discussion

4.1. Symmetric fission of $[Fe_4S_4X_4]^{2-} \rightarrow 2[Fe_2S_2X_2]^-$

The symmetric fission observed in the CID of $[Fe_4S_4X_4]^{2-}$ (X=Cl, Br, and SEt) was totally unexpected,

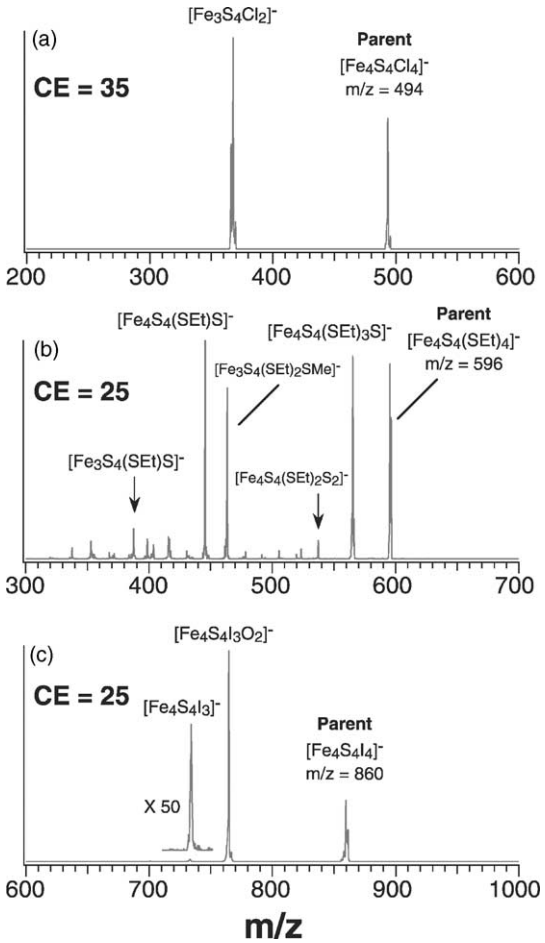

Fig. 5. CID of three singly-charged parent anions: (a) $[Fe_4S_4Cl_4]^-$, (b) $[Fe_4S_4(SEt)_4]^-$, and (c) $[Fe_4S_4I_4]^-$.

because it involved the breaking of four strong Fe–S bonds. Even more surprisingly, for $[Fe_4S_4Cl_4]^{2-}$ and $[Fe_4S_4Br_4]^{2-}$, the symmetric fission was the only CID channel. Why is it possible among so many other possible fragmentation channels, such as electron detachment or ligand elimination? These questions have been addressed in detail for $[Fe_4S_4Cl_4]^{2-}$ and $[Fe_4S_4Br_4]^{2-}$ in a recent publication, in which we combined PES studies of both the parents and the daughter anions and DFT calculations [40]. First of all, the intracluster coulomb repulsion due to the two excess charges in $[Fe_4S_4X_4]^{2-}$ must play a key role in the fission process, analogous to that in atomic nuclei [42] or multiply ionized metal clusters [43,44]. Intramolecular coulomb repulsion is unique to multiply-charged systems due to the presence of more than one excess charge in these systems. The importance of the coulomb repulsion for the fission process is shown vividly by the CID of the singly-charged $[Fe_4S_4X_4]^-$ anions (Fig. 5). The singly-charged parent anions have similar structure and bonding as the $[Fe_4S_4X_4]^{2-}$ dianions, but no symmetric fission was observed in their CID, due to the absence of the strong intracluster coulomb repulsion in these singly-charged systems. As reported previously [45], the magnitude of the intracluster coulomb repulsion can be obtained by estimating the repulsive coulomb barrier (RCB) of the multiply-charged anions from their photoelectron spectra. The RCB for removing an electron in $[Fe_4S_4X_4]^{2-}$ (X = Cl, Br, and SEt) was estimated to be ~2 eV [40]. The same amount of coulomb repulsion is available for the symmetric fission channel.

Further insight into the symmetric fission mechanisms was provided by considering the electronic structures of the $[Fe_4S_4X_4]^{2-}$ species. Broken-symmetry DFT calculations [10–12] showed that the $[Fe_4S_4]^{2+}$ core basically contains two valent-delocalized, ferromagnetically coupled $[Fe_2S_2]$ sub-layers, which in turn are antiferromagnetically coupled to give the low spin state. Thus the $[Fe_4S_4X_4]^{2-}$ clusters can be viewed as two ferromagnets aligned oppositely, but held together by the four strong Fe–S bonds. Hence, there is not only a strong intracluster coulomb repulsion, but also a strong magnetic repulsion in the $[Fe_4S_4X_4]^{2-}$ clusters. Both effects are critical for the symmetric fission. Our previous DFT calculations for $[Fe_4S_4Cl_4]^{2-}$ showed that the symmetric fission channel was nearly thermoneutral, consistent with the fact that no collision-induced electron detachment was observed because there is a substantial adiabatic electron detachment energy of 0.76 eV [40].

4.2. CID of $[Fe_4S_4(SEt)_4]^{2-}$ and $[Fe_4S_4I_4]^{2-}$: fission vs. electron detachment

Besides the symmetric fission channel, the observation of the singly-charged $[Fe_4S_4(SEt)_4]^-$ anion in the

CID of $[Fe_4S_4(SEt)_4]^{2-}$ (Fig. 3) was very interesting, suggesting that the electron loss channel was competitive with fission channel in this doubly-charged anion. Indeed, our PES data showed that $[Fe_4S_4(SEt)_4]^{2-}$ has a much lower adiabatic detachment energy (0.29 eV) [46] compared to that of $[Fe_4S_4Cl_4]^{2-}$ (0.76 eV). In addition, three small fragments were identified as $[Fe_2S_2(SEt)S]^-$, $[Fe_2S_2(SEt)]^-$, and $[FeS(SEt)_2]^-$ in the CID of $[Fe_4S_4(SEt)_4]^{2-}$, even at very low CE (Fig. 3b). The fragments could be produced either by multiple CID of the parent dianion $[Fe_4S_4(SEt)_4]^{2-}$ or by CID of the small amount of $[Fe_2S_2(SEt)_2]^-$ which existed in the initial isolated $m/z = 298$ mass peak. But the strong relative intensities of the isotopic peaks ($m/z = 296, 299$) of the fission product (Fig. 3c) indicated that most of the initial isolated mass species (>90%) should be the doubly-charged anion. Thus the dominant signals of the small fragments should be due to granddaughter anions of the parent dianions as a result of multiple CID, as follows:

$$[Fe_4S_4(SEt)_4]^{2-} \rightarrow 2[Fe_2S_2(SEt)_2]^- \rightarrow [Fe_2S_2(SEt)S]^- + Et \quad (1)$$

$$[Fe_4S_4(SEt)_4]^{2-} \rightarrow 2[Fe_2S_2(SEt)_2]^- \rightarrow [Fe_2S_2(SEt)]^- + SEt \quad (2)$$

$$[Fe_4S_4(SEt)_4]^{2-} \rightarrow 2[Fe_2S_2(SEt)_2]^- \rightarrow [FeS(SEt)_2]^- + FeS \quad (3)$$

The strong CE dependence of their relative intensities was consistent with the multiple CID processes. At high CE conditions (Fig. 3d), the dominant fragment is the loss of a C_2H_5 group from $[Fe_2S_2(SEt)_2]^-$, as given in Eq. (1).

Although we were not able to perform CID experiments for $[Fe_4S_4I_4]^{2-}$, we surmised that its dominant CID channel would be the electron detachment because only the singly-charged $[Fe_4S_4I_4]^-$ anion was observed on the LCQ apparatus from electrospray of a $(BTBA)_2[Fe_4S_4I_4]^{2-}$ sample (Fig. 4). This was a surprising observation since the adiabatic electron detachment energy of $[Fe_4S_4I_4]^{2-}$ (1.06 eV) [46] was even higher than that of $[Fe_4S_4Cl_4]^{2-}$ (0.76 eV). This result suggested that the electron loss channel in $[Fe_4S_4I_4]^{2-}$ must be extremely fissile. Therefore, we can conclude that there are only two competitive CID channels for all the $[Fe_4S_4X_4]^2$ doubly-charged complex anions in the gas phase: symmetric fission and electron detachment. The external ligand, X, seems to play a very important role in determining the CID patterns.

4.3. Ligand exchange reactions of $[Fe_4S_4X_4]^{2-}$ (X = Cl, Br, and I) with O_2

The observations of $[Fe_4S_4X_3O_2]^-$ in the CID experiments of $[Fe_4S_4X_4]^{2-}$ (X = Cl, Br, and I) were very interesting. During our experiments, the source part of the LCQ apparatus was purged with pure N_2 for at least 30 min before we took any mass spectrum. The concentration of O_2 in the background was expected to be very low. But strong $[Fe_4S_4X_3O_2]^-$ mass signals were observed during CID experiments of $[Fe_4S_4X_4]^{2-}$ (X = Cl, Br, and I), even during the initial ion storage (Figs. 2 and 4). This observation suggests that the ligand exchange reaction: $[Fe_4S_4X_4]^{2-} + O_2 \rightarrow [Fe_4S_4X_3O_2]^- + X^-$ must be extremely favorable. However, it was surprising that the $[Fe_4S_4(SEt)_4]^{2-}$ dianion seemed to be much more inert toward O_2 because there was no observable $[Fe_4S_4X_3O_2]^-$ signals in its CID spectra (Fig. 3). This ligand dependence toward O_2 in the $[Fe_4S_4X_4]^{2-}$ complexes was also an interesting observation. Since Fe–S proteins have been shown to be oxygen sensors [19–21], our current observation of the ligand exchange reaction between $[Fe_4S_4X_4]^{2-}$ and O_2 was interesting and may deserve further quantitative investigations in the future.

4.4. Symmetric fission in $[Fe_4S_4X_4]^{2-}$ and conversions between [4Fe4S] and [2Fe2S] in proteins

The symmetric fission channel can be viewed as a $[Fe_4S_4]$ to $[Fe_2S_2]$ conversion reaction in the gas phase. It is interesting to compare the gaseous process with a similar observation in the oxidized FNR protein in solution [19]. In the FNR protein, the

$[Fe_4S_4] \rightarrow [Fe_2S_2]$ conversion involves an oxidation reaction; the resulted [2Fe2S] cluster form of FNR has a fully oxidized state $[Fe_2S_2]^{2+}$ due to the exposure to O_2. The gas-phase symmetric fission channel is a non-redox reaction: the products remain the same oxidation state $[Fe_2S_2]^{+}$ as in the parent dianions. Because the fission product is exactly half of the parent cluster, one parent dianion $[Fe_4S_4X_4]^{2-}$ should generate two $[Fe_2S_2X_2]^{-}$ fragments. But in the solution reaction, two Fe^{2+} and two S^{2-} per cluster are lost during the conversion of the 4Fe to the 2Fe cluster. The ligand exchange reaction of the $[Fe_4S_4X_4]^{2-}$ complex with O_2, as discussed above, might be considered to be the first step of the disintegration from the [4Fe4S] to the [2Fe2S] state in FNR. In the history of Fe–S protein chemistry, the $[Fe_3S_4]^{+}$ cluster is the primary product of oxidation and one Fe^{2+} is obviously set free first. If this also holds for the 4Fe $\rightarrow$ 2Fe conversion, the $[Fe_3S_4]^{+}$ cluster would be an important intermediate in the degradation pathway. To confirm this mechanism, numerous attempts were made to detect the very easily observable EPR signals ($g = 2.01$) of the $[Fe_3S_4]^{+}$ clusters by rapid freezing during or after oxidation of anaerobically isolated FNR by air or ferricyanide, but never more than about 5% of the clusters originally present was observed to be in the 3Fe state [19]. Our observation of the 4Fe cluster symmetric fission in the gas phase may provide a new angle for the interpretation of the 4Fe $\rightarrow$ 2Fe conversion in FNR protein: the intracluster coulomb repulsion and the antiferromagnetic coupling may play an important role in this case and the two Fe and two S may depart the 4Fe cluster simultaneously, analogous to the gas-phase symmetric fission process.

5. Conclusions

A series of doubly-charged [4Fe4S] cluster anion, $[Fe_4S_4X_4]^{2-}$ (X = Cl, Br, I, and SC_2H_5), were produced in the gas phase by ESI and examined by tandem mass spectrometry in a quadrupole ion trap. Collision-induced dissociation channels of each dianion were analyzed by MS/MS experiments at different collision energies. For $[Fe_4S_4X_4]^{2-}$ (X = Cl, Br, and SC_2H_5), the dominant CID fragments were found to be symmetric fission to produce two $[Fe_2S_2X_2]^{-}$. Additionally, both collision-induced electron detachment and multiple CID of the fission daughter anions were observed for $[Fe_4S_4(SEt)_4]^{2-}$. For $[Fe_4S_4I_4]^{2-}$, collision-induced electron detachment was found to be the dominant CID channel even during the ion transport and storage, giving rise to the singly-charged cluster $[Fe_4S_4I_4]^{-}$. Our gas-phase experiments suggest that the solution phase conversion between the $[Fe_4S_4]$ and $[Fe_2S_2]$ assemblies in proteins may also involve related fission chemistry with reactive $[Fe_2S_2X_2]^{-}$ intermediates.

Acknowledgements

We thank Dr. C. Zhou from Professor R.H. Holm's group for providing us the $Fe_4S_4X_4{}^{2-}$ samples. We are grateful to Dr. R.J. Moore for his assistance in the CID experiments. This work was supported by the National Institutes of Health (GM-63555) and was performed at the W.R. Wiley Environmental Molecular Sciences Laboratory, a national scientific user facility sponsored by DOE's Office of Biological and Environmental Research and located at Pacific Northwest National Laboratory, which is operated for DOE by Battelle.

References

[1] H. Beinert, R.H. Holm, E. Munck, Science 277 (1997) 653.
[2] I. Bertini, S. Ciurli, C. Lunchinat, Struct. Bonding (Berlin) 83 (1995) 1.
[3] J.A. Ibers, R.H. Holm, Science 209 (1980) 223.
[4] R.H. Holm, J.A. Ibers, in: W. Lovenberg (Ed.), Iron–Sulfur Proteins, vol. III, Academic Press, New York, 1997, p. 205.
[5] H. Beinert, M.C. Kennedy, C.D. Stout, Chem. Rev. (Washington, DC) 96 (1996) 2335.
[6] H. Mastsubara, K. Saeki, in: R. Cammack (Ed.), Iron–Sulfur Proteins, Academic Press, San Diego, CA, 1992, p. 223.
[7] C.W. Carter Jr., J. Kraut, S.T. Freer, R.A. Alden, L.C. Sieker, E.T. Adman, L.H. Jensen, Proc. Natl. Acad. Sci. U.S.A. 69 (1972) 3526.

[8] J.M. Berg, R.H. Holm, in: T.G. Spiro (Ed.), Iron–Sulfur Protein, Wiley/Interscience, New York, 1982, p. 1.
[9] R.H. Holm, Acc. Chem. Res. 16 (1977) 2565.
[10] K.S. Hagen, J.G. Reynolds, R.H. Holm, J. Am. Chem. Soc. 103 (1981) 4054.
[11] R. Cammack, in: R. Cammack (Ed.), Iron–Sulfur Proteins, Academic Press, San Diego, CA, 1992, p. 281.
[12] P.J. Stephens, D.R. Jollie, A. Warshel, Chem. Rev. 96 (1996) 2491.
[13] L. Noodleman, E.J. Baerends, J. Am. Chem. Soc. 106 (1984) 2316.
[14] L. Noodleman, D.A. Case, Adv. Inorg. Chem. 38 (1992) 423.
[15] L. Noodleman, C.Y. Peng, D.A. Case, J.M. Mouesca, Coord. Chem. Rev. 144 (1995) 199.
[16] J.J.G. Moura, et al., J. Biol. Chem. 257 (1982) 6259.
[17] T.A. Kent, et al., Proc. Natl. Acad. Sci. U.S.A. 79 (1982) 1096.
[18] G.L. Anderson, J.B. Howard, Biochemistry 23 (1984) 2118.
[19] N. Khoroshilova, C. Popescu, E. Münck, H. Beinert, P.J. Kiley, Proc. Natl. Acad. Sci. U.S.A. 94 (1997) 6087.
[20] N. Khoroshilova, H. Beinert, P.J. Kiley, Proc. Natl. Acad. Sci. U.S.A. 92 (1995) 2499.
[21] C.V. Popescu, D.M. Bates, H. Beinert, E. Münck, P.J. Kiley, Proc. Natl. Acad. Sci. U.S.A. 95 (1998) 13431.
[22] I.A. Papayannopoulos, Mass Spectrom. Rev. 14 (1995) 49.
[23] S.E. Martin, J. Shabanowitz, D.F. Hunt, J.A. Marto, Anal. Chem. 72 (2000) 4266.
[24] C. Masselon, G.A. Anderson, R. Harkewicz, J.E. Bruce, L. Pasa-Tolic, R.D. Smith, Anal. Chem. 72 (2000) 1918.
[25] J.A. Loo, C.G. Edmonds, R.D. Smith, Science 248 (1990) 201.
[26] Q.Y. Wu, S. Vanorden, X.H. Cheng, R. Bakhtiar, R.D. Smith, Anal. Chem. 67 (1995) 2498.
[27] J.L. Stephenson, B.J. Cargile, S.A. McLuckey, Rapid Commun. Mass Spectrom. 13 (1999) 2040.
[28] N.L. Kelleher, H.Y. Lin, G.A. Valaskovic, D.J. Aaserud, E.K. Fridriksson, F.W. Mclafferty, J. Am. Chem. Soc. 121 (1999) 806.
[29] R.A. Zubarev, D.M. Horn, E.K. Fridriksson, N.L. Kelleher, N.A. Kruger, M.A. Lewis, B.K. Carpenter, F.W. McLafferty, Anal. Chem. 72 (2000) 563.
[30] G.E. Reid, J. Wu, P.A. Chrisman, J.M. Wells, S.A. McLuckey, Anal. Chem. 73 (2001) 3274.
[31] V.N. Reinhold, B.B. Reinhold, C.E. Costello, Anal. Chem. 67 (1995) 1772.
[32] T. Solouki, B.B. Reinhold, C.E. Costello, M. O'Malley, S.H. Guan, A.G. Marshall, Anal. Chem. 70 (1998) 857.
[33] D.J. Harvey, J. Mass Spectrom. 35 (2000) 1178.
[34] D. Zhang, R.G. Cooks, Int. J. Mass Spectrom. 195/196 (2000) 667.
[35] M.P. Ince, B.A. Perera, M.J. Van Stipdonk, Int. J. Mass Spectrom. 207 (2001) 41.
[36] S.A. McLuckey, G.L. Glish, G.J. Vanberkel, Int. J. Mass Spectrom. Ion Process. 106 (1991) 213.
[37] E.M. Raymond, J. Mass Spectrom. 32 (1997) 351.
[38] X.B. Wang, L.S. Wang, J. Chem. Phys. 112 (2000) 6959.
[39] X. Yang, X.B. Wang, Y.J. Fu, L.S. Wang, J. Phys. Chem. A 107 (2003) 1703.
[40] X. Yang, X.B. Wang, S.Q. Niu, C.J. Pickett, T. Ichiye, L.S. Wang, Phys. Rev. Lett. 89 (2002) 163401.
[41] L.S. Wang, C.F. Ding, X.B. Wang, S.E. Barlow, Rev. Sci. Instrum. 70 (1999) 1957.
[42] N. Bohr, J.A. Wheeler, Phys. Rev. 56 (1939) 426.
[43] U. Naher, S. Bjorholm, S. Frauendorf, F. Garcias, C. Guet, Phys. Rep. 285 (1997) 245.
[44] C. Brechignac, Ph. Cahuzac, F. Carlier, M. de Frutos, Phys. Rev. Lett. 64 (1990) 2893.
[45] L.S. Wang, C.F. Ding, X.B. Wang, J.B. Nicholas, Phys. Rev. Lett. 81 (1998) 2667.
[46] X.B. Wang, X. Yang, L.S. Wang, unpublished results.